Coherent Method for Radio-Frequency Measurement of Distance between Antennas

Nenad Vukmirović, Miloš Janjić, Nikola Basta, and Miljko Erić

***Abstract*—The paper proposes a coherent method for radio-frequency measurement of the effective distance between two antennas. A transmitter sends a known waveform to a receiver, which processes the received signal to estimate its delay. The two transceivers are mutually synchronized, but different sources of delays/phase shifts still remain. A calibration step enables the system to estimate the total delay including the delays in the antennas. Differential measurements with three antennas enable us to estimate the delays in the antennas, which can be used as correction factors in measurements of the effective distance without the nuisance delays. The results of experiments performed on a prototype system, built of off-the-shelf equipment, show the consistency and the variance of the estimates. This method could be used to measure the geometry of a distributed array during its deployment, for the purposes of localization.**

***Index Terms*—Precise antenna positioning; coherent delay estimation; Universal Software Radio Peripheral; calibration; differential measurement**

I. Introduction

THIS paper proposes a radio-wave-based method for measuring the distance between two antennas and provides the results of experimental verification.

An approach for precise positioning of antennas in an ultra-wideband (UWB) system for indoor self-localization was discussed in [1]. It was found that a major source of localization error were the errors in the positions of the system's antennas. If the distance for each pair of antennas were measured accurately, the geometry of the distributed antenna array could be inferred and used for accurate localization. However, one should carefully consider which point of an antenna is the one that correctly represents it (the referent point). The best point is the one from which the radio wave propagates directly outward at the radio frequency which the antenna will be used for. This point is the antenna phase center. This complicates physical-distance measurements because the phase center may well be inside the body of the antenna (inaccessible for fine mechanical measurements) and it generally depends on the frequency as explained in [2], [3], [4]. These papers discuss measurement methods of the coordinates of an antenna's phase center and the complications that arise.

We propose a method based on RF (Radio Frequency) transmission and signal processing, which estimates the inter-antenna distance. This distance naturally corresponds to the phase centers and we call it the *effective distance*. Additionally, this allows us to circumvent the measurement of phase center positions and the complications associated with fine mechanical measurements of the distance between them. This represents an extension of the work in [5], which proposed a method for effective distance estimation based on group-delay and provided simulation results for different antenna orientations.

The paper [6] presented a method for coherent measurement of the distance between antennas (and the clock drift of their front-ends) up to an additive constant. We build on this idea by proposing a method that is also coherent, but is able to measure the absolute distance, thanks to a special calibration step and additional differential measurements that allow us to compensate for unwanted delays in the hardware, while having less stringent requirements on the synchronization of the front-ends. We use off-the-shelf equipment, including USRP (Universal Software Radio Peripheral) devices.

Coherent delay estimation, although potentially a lot more accurate than non-coherent methods, has an inherent ambiguity problem. Namely, the estimation error is a sum of an integral and fractional

N. V., M. J., N. B., and M. E. are with the University of Belgrade, School of Electrical Engineering, Serbia

N. V. and M. J. are also with the Innovation Center of School of Electrical Engineering, University of Belgrade, Serbia

M. E. is also with Vlatacom Institute, Belgrade, Serbia

This paper is a result of the research supported by the Serbian Ministry of Education, Science and Technological Development.

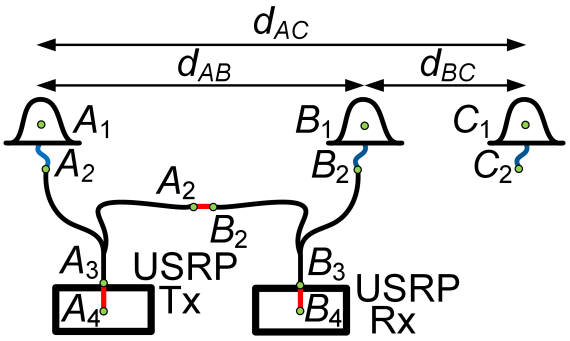

Fig. 1. The measurement setup with two USRP devices (Tx and Rx).

multiple of the carrier wavelength, the integral part representing the ambiguity. Even though the fractional error can be very small, applications that rely on accurate total distance measurements require the ambiguity to be resolved. The paper [7], although for a completely different setup (optical measurement), also has a method with the same error structure (see Sec. 2.3) and proposes a sophisticated method for resolving the ambiguity. In our paper we use a very coarse (and, therefore, simple) mechanical measurement of distance to resolve the ambiguity.

The most important application of the proposed method is measuring the (arbitrary) geometry of a distributed antenna system, for use in coherent localization [8], [9], which in turn can be used to improve the link performance of wireless systems, [10], by means of distributed beamforming or spatial multiplexing, to name a few.

II. Problem formulation

One USRP (Tx) transmits a predefined periodic waveform and another (Rx) receives the signal, which is then processed (see Fig. 1). One period of the waveform is determined by a vector of samples (a sequence), denoted by $\mathbf{s} = [s_0, s_1, \ldots, s_{N-1}]^\top$. Sequence $\mathbf{s}$ is a priori known at the Rx side and the processor estimates its delay with respect to the local Rx time axis.

The estimate is coherent, which means that the information is extracted not only from the signal envelope, but also from the carrier phase. This relies on the fact that when the delay of a signal in the RF domain increases by some $\Delta\tau$, the envelope is time-shifted by $-\Delta\tau$ and the carrier phase by $-\omega_\mathrm{c}\Delta\tau$ (their shifts are coupled), where $\omega_\mathrm{c} = 2\pi f_\mathrm{c}$ is the carrier frequency.

Due to the restrictions of the off-the-shelf equipment used in the measurements, we have to consider different kinds of sources of error. A coherent algorithm requires the USRPs to be frequency synchronized. However, phase errors remain due to discrepancies in the lengths of the paths for the frequency reference (from a common source) in the two front-ends and the phase-locked loops (PLLs). There are also delays in the front-ends to (or from) the referent points in the chassis RF connectors (A_4A_3 and B_3B_4 in Fig. 1), in the signal cables between these connectors and the antenna connectors (A_3A_2 and B_2B_3), and between these and the referent points in the antennas (A_2A_1 and B_1B_2). Points A_1 and B_1 are not necessarily the phase centers of the antennas (in many antennas phase centers are not uniquely defined), but are chosen as geometrical reference points of antennas A and B. The algorithm considers that an RF wave propagates in free space between these points.

There is also a mismatch between the Tx and Rx local time axes, denoted by t_0. We wish to estimate the effective distance between antennas A and B, denoted by $d_{AB} = d(A_1B_1)$. We convert between delays and effective distances as $d_{AB} = c\tau_{AB}$, where c is the *free-space* propagation velocity of an RF wave at the given carrier frequency (by convention).

A phase drift exists, but its mean value is 0 and its variance is negligible because the propagation distances in the experiment are relatively short. There is also the clock drift, $\tau_\mathrm{clk}(t)$, which can accumulate over time (its mean is not 0) because of independent clock generators in USRPs, but it only impacts the signal envelope. There can also be frequency-selective attenuation (e.g. due to anti-aliasing filters, coaxial cables, A/D or D/A converters...), which we separate into two factors – a delay (phase and time delay) and a waveform distortion factor (modeled by an unknown impulse response $h(t)$). Accounting for all these effects, we can write the model of the received signal, $u(t)$, as

$$\begin{aligned} u(t) =& s_\mathrm{r}(t) + \eta(t) \\ s_\mathrm{r}(t) =& a\mathrm{e}^{-\mathrm{j}(\omega_\mathrm{c}\tau_\mathrm{a}+\varphi)}\,(h * s)\,(t - \tau_\mathrm{a} - \tau_\mathrm{clk}(t)), \end{aligned} \quad (1)$$

where τ_a is the total constant envelope delay (which also includes the Tx t-axis shift t_0), $\omega_\mathrm{c}\tau_\mathrm{a} + \varphi$ is

the total constant phase delay, $(h * s)(\cdot)$ is the convolution of the transmitted signal $s(t)$ with the impulse response $h(t)$ (modeling the effects in the entire path form the D/A converter in Tx to the A/D converter in Rx), $\tau_{\text{clk}}(t)$ is a process that slowly varies over time, a is a positive real-valued amplitude coefficient and $\eta(t)$ includes noise, multipath propagation and interference.

Note that we have normalized frequency values by the sampling frequency, $\widetilde{f}_{\text{s}}$, and time values by the sampling interval, $1/\widetilde{f}_{\text{s}}$, so that we can simply write $s(t) = s_t$, $t \in \{0, 1, \ldots, N-1\}$ (a convenient way to switch between the analog and the digital domain). This, however, does *not* restrict the argument for $s(\cdot)$ to a set of integers – $s(t)$ is still a continuous waveform. This also implies that c is normalized such that $c = \widetilde{c}/\widetilde{f}_{\text{s}}$ and has a unit [m/sample], where $\widetilde{c} = 3 \cdot 10^8$ m/s. If we need to explicitly write a parameter in physical units, we will use the symbol $\widetilde{\ }$ above it (e.g. $\widetilde{f}_{\text{c}} = 1.2$ GHz).

Since the estimation algorithm (described in Sec. III) is robust against the effects of $h(t)$, we will omit it. Also, since the algorithm is coherent, it perceives the phase delay φ as a time delay equal to $\varphi/\omega_{\text{c}}$. So, by substituting $\tau = \tau_{\text{a}} + \varphi/\omega_{\text{c}}$, we get a simplified model of the useful signal $s_{\text{r}}(t)$:

$$s_{\text{r}}(t) \approx a\text{e}^{-\text{j}\omega_{\text{c}}\tau} s(t - \tau - \tau_{\text{e}}(t)), \tag{2}$$

where τ is the total constant delay (for both the envelope and phase) and $\tau_{\text{e}}(t) = \tau_{\text{clk}}(t) - \varphi/\omega_{\text{c}}$ is the excess envelope-only delay (a slowly varying process).

III. The Measurement Method

A basic measurement consists of acquiring a signal segment of N samples, given by

$$\mathbf{u} = [u(0), u(1), \ldots, u(N-1)]^{\top} \tag{3}$$

and estimating the delay of the sequence **s** within that segment by the GCC-type (Generalized Cross-Correlation) delay-estimation algorithm given in [8],

$$\widehat{\tau} = \underset{\tau \in [0,N)}{\arg\max}\, \text{Re}\left(\mathbf{u}^{\text{H}} \mathbf{s}_{-\tau}\right) \tag{4}$$

where $\mathbf{s}_{-\tau} = \text{e}^{\text{j}\omega_{\text{c}}\tau}\,[s(\tau), s(\tau+1), \ldots, s(\tau+N-1)]^{\top}$ is a vector of samples of the waveform $s(t)$ time-shifted by τ (or delayed by $-\tau$) *including* the coupled carrier phase shift, Re denotes the real part, $^{\top}$ matrix transpose, and $^{\text{H}}$ conjugate transpose. Since $s(t)$ is periodic with period N, a regular time shift is the same as a cyclic time shift, thus we can compute $\mathbf{s}_{-\tau}$ using DFT (Discrete Fourier Transform) as

$$\mathbf{s}_{-\tau} = \mathbf{F}^{\text{H}} \mathbf{D}_{-\tau} \mathbf{F} \mathbf{s}, \tag{5}$$

$$\mathbf{F} = 1/\sqrt{N}\exp(-\text{j}2\pi/N \cdot \mathbf{k}\mathbf{n}^{\top}), \tag{6}$$

$$\mathbf{D}_{-\tau} = \exp(\text{j}\omega_{\text{c}}\tau)\,\text{Diag}\left\{\exp(\text{j}2\pi/N \cdot \mathbf{k}\tau)\right\}, \tag{7}$$

$$\mathbf{n} = [0, 1, \ldots, N-1]^{\top}, \tag{8}$$

$$\mathbf{k} = [-N/2, -N/2+1, \ldots, N/2-1]^{\top}. \tag{9}$$

F is a modified DFT matrix such that $\mathbf{F}^{-1} = \mathbf{F}^{\text{H}}$, so a numerically more efficient form of (4) is

$$\widehat{\tau} = \underset{\tau \in [0,N)}{\arg\max}\, \text{Re}\left(\mathbf{U}^{\text{H}} \mathbf{D}_{-\tau} \mathbf{S}\right), \tag{10}$$

where $\mathbf{U} = \mathbf{F}\mathbf{u}$ and $\mathbf{S} = \mathbf{F}\mathbf{s}$ are computed only once in preprocessing.

A. Type-I Measurement

In the *antenna configuration* in Fig. 1, in which the signal cables A_3A_2 and B_2B_3 are connected to the antennas, a basic measurement provides an estimate

$$\widehat{\tau}_{\text{ant}} = \tau_{\text{ses}} + \tau_A + \tau_{AB} + \tau_B + \varepsilon_{\text{ant}}, \tag{11}$$

where τ_A is the delay in antenna A (from A_2 to A_1), τ_B in antenna B (i.e. B_1B_2), τ_{ses} is the combined effect of the signal cables and front-ends, and ε_{ant} is the error.

The delay τ_{ses} is preserved within one driver session with the USRP devices (if we neglect the effects of the drift $\tau_{\text{e}}(t)$), but it takes a new value (changes unpredictably) each time a new session starts. Therefore, we can perform another basic measurement within *the same* driver session, but in the *guided configuration* (see Fig. 1), in which the signal cables are connected to each other by a short connector of effective length $L = c\tau_L$ (between A_2 and B_2). We get an estimate

$$\widehat{\tau}_{\text{g}} = \tau_{\text{ses}} + \tau_L + \varepsilon_{\text{g}}, \tag{12}$$

where ε_{g} is the error. From (11) and (12) we get

$$\tau_{AB} = \widehat{\tau}' - \tau_A - \tau_B + \tau_L + \varepsilon', \tag{13}$$

where $\widehat{\tau}' = \widehat{\tau}_{\text{ant}} - \widehat{\tau}_{\text{g}}$, $\varepsilon' = \varepsilon_{\text{g}} - \varepsilon_{\text{ant}}$ is the combined error. Note that we can perform multiple basic measurements in each of the two configurations to get more accurate estimates of $\widehat{\tau}_{\text{ant}}$ and $\widehat{\tau}_{\text{g}}$, thanks to averaging. Also, since the drift in $\tau_{\text{e}}(t)$ accumulates over time, by making the session shorter, i.e. if we change the configurations (disconnect and reconnect the cables) more quickly, the negative effect of $\tau_{\text{e}}(t)$ is expected to be smaller. Taking multiple measurements can also be useful as a way to diagnose this negative effect, especially if they are spread out across the interval of the session, because this effect is expected to grow over time.

We call the procedure of acquiring one or more $\widehat{\tau}_{\text{ant}}$ and one or more $\widehat{\tau}_{\text{g}}$ estimates, all within the same driver session, a type-I measurement.

B. Type-II Measurement

We can obtain τ_L in (13) in a fine measurement by some external means, but the terms τ_A and τ_B remain unsolved. We propose to use antenna C, with the referent point C_1, such that A_1, B_1, and C_1 are colinear as in Fig. 1. In that setup, we would perform a type-I measurement with antennas A and B and another with B and C. We would then remove the antenna B, so that it does not block the propagation from A to C and perform a type-I measurement with A and C. As a result, we get

$$\tau_{AB} = \widehat{\tau}'_1 - \tau_A - \tau_B + \tau_L + \varepsilon'_1, \quad (14)$$
$$\tau_{BC} = \widehat{\tau}'_2 - \tau_B - \tau_C + \tau_L + \varepsilon'_2, \quad (15)$$
$$\tau_{AC} = \widehat{\tau}'_3 - \tau_A - \tau_C + \tau_L + \varepsilon'_3. \quad (16)$$

Relying on $\tau_{AB} + \tau_{BC} = \tau_{AC}$, we get an estimate of τ_B as

$$\widehat{\tau}_B = \tau_B + \varepsilon'' = \left(\widehat{\tau}'_1 + \widehat{\tau}'_2 - \widehat{\tau}'_3 + \tau_L\right)/2. \quad (17)$$

where ε'' is the combined error. We call this procedure of obtaining $\widehat{\tau}_B$ a type-II measurement.

Note that $\widehat{\tau}_B$ is independent of the distances between the antennas and the delays in antennas A and C, for fixed signal-to-noise ratios, as long as the antennas are in the far-field regions of one another. Additionally, a deviation of B_1 from the line A_1C_1 influences ε'' as a second-order infinitesimal, so this deviation can be neglected.

Type-II measurements can be performed for each of the antennas in an RF anechoic chamber before they are deployed. Once deployed, the estimates $\widehat{\tau}_A$, $\widehat{\tau}_B$, ... can be input into (13) as correction factors, providing

$$\widehat{\tau}_{AB} = \widehat{\tau}' - \widehat{\tau}_A - \widehat{\tau}_B + \widehat{\tau}_L. \quad (18)$$

This way we get an estimate of the effective electrical distance between A and B, $\widehat{d}_{AB} = c\widehat{\tau}_{AB}$, or any other pair of antennas we use to form a distributed antenna array. As a result, the antennas can be placed arbitrarily and then the geometry of the array can be *measured*, by multiple type-I measurements (with appropriate correction factors).

C. Integral and fractional errors

In each of these measurements, the error (such as ε' in (13)) has two components – the first is an integer multiple of the carrier cycle, $1/f_{\text{c}}$, for delays, or the carrier wavelength, $\lambda_{\text{c}} = c/f_{\text{c}}$, for lengths, and the second component is the fractional part (the remainder, which is usually a few orders of magnitude smaller than λ_{c}):

$$\begin{aligned} \varepsilon' &= m/f_{\text{c}} + \varepsilon'_{\text{frac}}, \text{ for delays} \\ c\varepsilon' &= m\lambda_{\text{c}} + c\varepsilon'_{\text{frac}}, \text{ for distances}, \end{aligned} \quad (19)$$

for some $m \in \mathbb{Z}$. The presence of $m\lambda_{\text{c}}$ is known as the (integer wavelength) ambiguity problem and it is characteristic of coherent delay algorithms [11], [12]. This effect occurs because an RF signal and its replica delayed by $1/f_{\text{c}}$ closely resemble each other. The term $\tau_{\text{e}}(t)$ increases the error, but mostly its integral part (the ambiguity). Even though the integral part of the error is usually much larger, it is not as important as the $\varepsilon'_{\text{frac}}$ part. For example, the performance of distributed beamforming is deteriorated mostly by $\varepsilon'_{\text{frac}}$ and very little by the ambiguity.

We propose to solve the ambiguity problem by taking a rough estimate of the distance, d_{AB}, by some external means (mechanical means, laser range finder, or even an RF measurement but at a different carrier frequency). That method only has to be accurate enough to correctly resolve m (e.g., at $\widetilde{f}_{\text{c}} = 1$ GHz, $\lambda_{\text{c}} = 30$ cm, an accuracy of a few centimeters would suffice).

Finally, the effective lengths/distances of the guided parts of the system can depend on $\widetilde{f}_{\text{c}}$, so care should be taken to measure them at different

Fig. 2. The experiment environment.

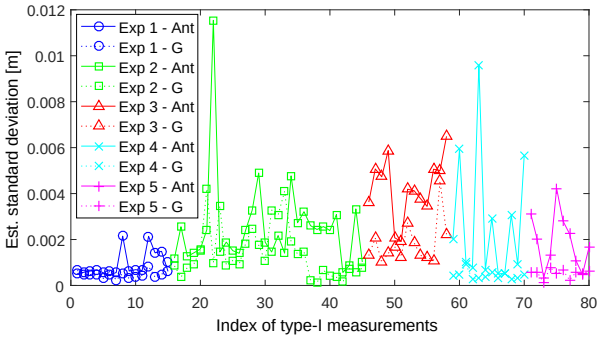

Fig. 3. Estimated standard deviations of lengths obtained within different type-I measurements.

frequencies and later use the correction factors at the correct frequency.

IV. Results of Measurements

We performed experiments with n210 USRP devices with omnidirectional antennas (connected by 25 m long coaxial cables) in an outdoor urban environment in front of the Innovation Center of the School of Electrical Engineering in Belgrade (Fig. 2). Most of the type-I measurements consisted of 8 and 4 basic measurements in the antenna and guided configuration, respectively. To reduce the bias in the estimates, we did not use an attenuator to connect A_2 and B_2. Thus, the Rx signal level was significantly lower in the antenna configuration than in the guided one. So, we used a greater number of measurements (8) in the antenna configuration to compensate for higher error variance. We performed multiple different experiments as a proof-of-concept.

In experiment (exp.) 1, we performed a type-II measurement with antennas A, B, and C in a line in that order, at $\widetilde{f}_{\mathrm{c}} = 990$ MHz. There were 5 type-I measurements for each pair of antennas (AB, BC, and AC). Fig. 3 shows standard deviations, σ_{A} and σ_{G}, of the effective length estimates in the antenna and guided configuration, respectively, within each type-I measurement. In this section, we concentrate on the std. deviations of the fractional part $c\varepsilon'_{\mathrm{frac}}$ from (19) (throughout these experiments, the std. deviations of the ambiguity m in (19) were grouped around 1 and most of them were in the range between 0 to 3). In most cases, σ_{A} was greater than σ_{G}, as expected, and both were less than 7 mm. The resulting 3 groups of estimates (one for each antenna pair) had standard deviations 1.5 mm, 3.5 mm, and 2.9 mm, as shown in Table I. The final (type-II) estimate of exp. 1 (the effective length of antenna B) was $L_B = 54.94$ cm, according to (17). (This was expected because the physical length of B_1B_2 was around 40 cm, with a roughly 1.5 times lower propagation velocity.) Note that this was a two-stage averaging, which made the total number of basic measurements 120 (antenna) and 60 (guided) for this single type-II estimate.

TABLE I
Parameters of experiments and standard deviations (σ).

Exp.	Type	Ant. pair	No. of meas.	σ [mm]	$\sigma/\lambda_{\mathrm{c}}$
1	II	AB	5	1.5	0.005
		BC	5	3.5	0.012
		AC	5	2.9	0.0096
2	II	AB	10	7.7	0.025
		BC	10	2.4	0.008
		AC	10	7.8	0.026
3	II	AB	5	9.3	0.034
		BC	4	3.9	0.014
		AC	4	3	0.011
4	II	BA	4	7.6	0.025
		AC	4	2.6	0.0086
		BC	4	11.3	0.037
5	I	AB	10	5.6	0.018

To reduce the number of times the cables had to be disconnected/reconnected to a half (less wear-and-tear of connectors), we started one type-I measurement in the antenna configuration and ended it in the guided one, and then reversed the order in the next measurement. We continued alternating this order throughout the campaign. Another advantage

of this was to partially compensate for the bias created by a clock drift growing in one direction over the course of a driver session. The expected effect of this was an increase in σ of type-I estimates for each pair of antennas and a decrease in the bias in the final estimate of the pair.

To test the repeatability of measurement, exp. 2 was with the same antennas and $\widetilde{f}_\mathrm{c}$ as in exp. 1, but in different conditions – different weather conditions (day) and inter-antenna distances. There were 10 type-I measurements for each antenna pair and the σ values of each pair (as well as the ones for the rest of the experiments in this section) are given in Table I. For individual type-I σ values, see Fig. 3. The final estimate was $L_B = 55.08$ cm.

To test the consistency across the frequencies, exp. 3 was carried out with the same setup as exp. 2, but at $\widetilde{f}_\mathrm{c} = 1.1$ GHz (in this experiment only). Note that the effective length B_1B_2 (L_B) was not expected to be identical at these two frequencies (even though the physical one was). The final estimate was $L_B = 56.04$ cm.

In exp. 4 the antennas were placed as B-A-C (antenna A in the middle), with the goal of estimating L_A. The final estimate was $L_A = 66.68$ cm.

Exp. 5 consisted of 10 type-I measurements with antennas A and B, but with correction factors from exps. 2 and 4 (using (18)). The aim was to estimate the effective distance between the referent points of these antennas (i.e., in the air only), L_{AB}. According to a mechanical measurement, the distance was 3.45 m. The resulting individual σ values are given in Fig. 3 and the σ value of the final result in Table I. The final estimate was $d_{AB} = 3.32$ m.

In future work, one might consider decreasing the difference in the Rx signal levels in the antenna and guided configuration, in order to reduce the influence of thermal and quantization noise, but without inducing a bias in the delay estimation. Furthermore, compensation of the remaining bias in the estimates is also of interest. Additionally, (dis)connecting cables manually is impractical for deployments of distributed antenna arrays, so the switching (between configurations) may be designed so it would be electronically controlled and automatic, thus decreasing the probability of human error in the experiment.

V. Conclusion

In this paper we proposed a method for measuring electronically the effective distance between a pair of antennas. A prototype was built of off-the-shelf equipment. The results of the field tests showed the potential of the presented method, as well as the aspects that require improvement in order to use it in deploying distributed antenna arrays with subwavelength accuracy. Such a method can have a great impact on future wireless systems as an enabler for coherent localization.

References

[1] M. Erić, R. Zetik, and D. Vučić, "An approach for determination of antenna positions in distributed antenna system used for UWB indoor self-localization: Experimental results," in *2013 21st Telecommunications Forum Telfor (TELFOR)*, 2013, pp. 204–207.

[2] H. Yuan, H. Liu, J. Jia, T. Su, and C. Zeng, "A novel algorithm to compute 3d phase center," *Electromagnetics*, vol. 40, no. 7, pp. 486–499, 2020.

[3] P. N. Betjes, "An algorithm for automated phase center determination and its implementation," in *AMTA*, 2007, pp. 190–195.

[4] C. Esposito, A. Gifuni, and S. Perna, "Measurement of the antenna phase center position in anechoic chamber," *IEEE Antennas and Wireless Propagation Letters*, vol. 17, no. 12, pp. 2183–2187, 2018.

[5] N. Basta and M. Erić, "Method for estimation of electrical distance between antennas based on music-type algorithm," in *7th International Conference on Electrical, Electronics and Computing Engineering (IcETRAN 2020)*, 2020, pp. 1–4.

[6] P. Bidigare, S. Pruessing, D. Raeman, D. Scherber, U. Madhow, and R. Mudumbai, "Initial over-the-air performance assessment of ranging and clock synchronization using radio frequency signal exchange," in *2012 IEEE Statistical Signal Processing Workshop (SSP)*, 2012, pp. 1–4.

[7] G. Tang, X. Qu, F. Zhang, X. Zhao, and B. Peng, "Absolute distance measurement based on spectral interferometry using femtosecond optical frequency comb," *Optics and Lasers in Engineering*, vol. 120, pp. 71–78, 2019.

[8] N. Vukmirović, M. Janjić, P. M. Djurić, and M. Erić, "Position estimation with a millimeter-wave massive MIMO system based on distributed steerable phased antenna arrays," *EURASIP Journal on Advances in Signal Processing*, vol. 2018, no. 1, p. 33, 2018.

[9] N. Vukmirović, M. Erić, M. Janjić, and P. M. Djurić, "Direct wideband coherent localization by distributed antenna arrays," *Sensors*, vol. 19, no. 20, p. 4582, 2019.

[10] R. Di Taranto, S. Muppirisetty, R. Raulefs, D. Slock, T. Svensson, and H. Wymeersch, "Location-aware communications for 5G networks: How location information can improve scalability, latency, and robustness of 5G," *IEEE Signal Processing Magazine*, vol. 31, no. 6, pp. 102–112, 2014.

[11] A. J. Weiss and E. Weinstein, "Fundamental limitations in passive time delay estimation – part I: Narrow-band systems," *IEEE Transactions on Acoustics, Speech, and Signal Processing*, vol. 31, no. 2, pp. 472–486, 1983.

[12] E. Weinstein and A. J. Weiss, "Fundamental limitations in passive time delay estimation – part II: Wide-band systems," *IEEE Transactions on Acoustics, Speech, and Signal Processing*, vol. 32, no. 5, pp. 1064–1078, 1984.